SIAM J. APPL. MATH.
Vol. 74, No. 6, pp. 1852–1869

TWO-DIMENSIONAL WAVE PROPAGATION IN LAYERED PERIODIC MEDIA*

MANUEL QUEZADA DE LUNA† AND DAVID I. KETCHESON‡

Abstract. We study two-dimensional wave propagation in materials whose properties vary periodically in one direction only. High-order homogenization is carried out to derive a dispersive effective medium approximation. One-dimensional materials with constant impedance exhibit no effective dispersion. We show that a new kind of effective dispersion may arise in two dimensions, even in materials with constant impedance. This dispersion is a macroscopic effect of microscopic diffraction caused by spatial variation in the sound speed. We analyze this dispersive effect by using high-order homogenization to derive an anisotropic, dispersive effective medium. We generalize to two dimensions a homogenization approach that has been used previously for one-dimensional problems. Pseudospectral solutions of the effective medium equations agree to high accuracy with finite volume direct numerical simulations of the variable-coefficient equations.

Key words. wave propogation, periodic media, effective dispersion, diffraction, homogenization

AMS subject classifications. 35B27, 35L45, 35P25

DOI. 10.1137/130937962

1. Introduction.

Consider the propagation of acoustic waves in a two-dimensional medium whose properties vary in one coordinate direction (say, y). Such waves are described by the PDE

$$p_{tt} = K(y)\nabla \cdot \left(\frac{1}{\rho(y)}\nabla p\right). \tag{1}$$

Here $p = p(x, y, t)$ is the pressure, $K(y)$ is the bulk modulus, and $\rho(y)$ is the material density. We focus on the initial value problem in an unbounded spatial domain. We are interested in materials whose spatial variation is periodic:

$$K(y + \Omega) = K(y), \qquad \rho(y + \Omega) = \rho(y).$$

Here Ω denotes the period. In all numerical experiments and plots, we set $\Omega = 1$.

A simple example of such a medium is shown in Figure 1. We refer to these as *layered* materials, though the coefficients need not be piecewise-constant. In subsequent sections, we frequently use the terms *normal propagation* and *transverse propagation* to refer to propagation normal to or parallel to the axis of homogeneity, respectively (see Figure 1).

We consider the propagation of waves with characteristic wavelength λ over a distance L in a periodic medium with period Ω, where

$$\Omega < \lambda \ll L.$$

Because the wavelength λ is larger than the material period Ω, the waves "see" the medium as nearly homogeneous and travel at an effective velocity related to averages

*Received by the editors September 23, 2013; accepted for publication (in revised form) August 21, 2014; published electronically December 3, 2014.
http://www.siam.org/journals/siap/74-6/93796.html
†Department of Mathematics, Texas A&M University, College Station, TX 77843 (mquezada@math.tamu.edu).
‡Division of Computer, Electrical and Mathematical Sciences, 4700 King Abdullah University of Science and Technology (KAUST), Thuwal, 23955-6900, Kingdom of Saudi Arabia (david.ketcheson@kaust.edu.sa).

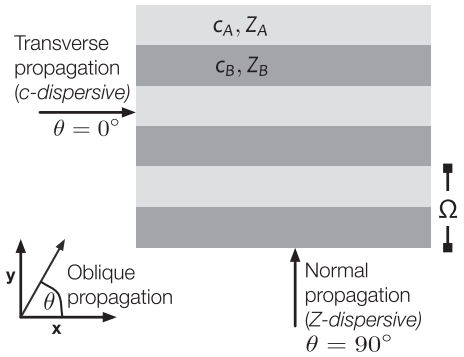

FIG. 1. *Wave propagation in a layered periodic medium. The material shown is repeated periodically in y and extends infinitely in both coordinate directions. A piecewise-constant medium is shown for simplicity, but arbitrary periodic variation (in y) is considered. The terms* normal *and* transverse *are used throughout this work to denote propagation in the y and x coordinate directions, respectively.*

of the material properties. The study of wave propagation in this regime has been the subject of much study; see [2, 5] and references therein. Many works focus exclusively on the lowest-order terms in the homogenized equations. The potential for dispersive higher-order terms due to material periodicity was derived using Bloch expansions in [12] and computed explicitly for the case of a one-dimensional layered medium. Later works have also studied effective dispersion in one-dimensional periodic media and further developed the relevant high-order homogenization techniques for time-dependent problems [4, 1, 3, 14].

The motivation for the present work comes from the discovery of a new kind of effective dispersion, which is described and demonstrated briefly in the rest of the introduction. In section 2 we derive an effective medium approximation to the variable-coefficient wave equation (1). The technique we use is an extension of those appearing in [1, 14, 10]. This seems to be the first explicit application of such high-order homogenization to multidimensional materials. In section 3 we explore the dispersion relation implied by the effective medium equations, showing that the effective medium is anisotropic and dispersive. In section 4, we examine the complementary roles played by variation in the impedance and the sound speed. We also validate our homogenized model by comparing pseudospectral solutions of the effective medium equations with finite volume direct simulations of the variable-coefficient wave equation (1).

All code used for computations in this work, along with Mathematica worksheets used to derive the homogenized equations, are available at http://github.com/ketch/effective_dispersion_RR.

1.1. Effective dispersion in a layered medium. The qualitative behavior of waves propagating in a periodic medium depends on whether the sound speed $c(y) = \sqrt{K/\rho}$ and the impedance $Z(y) = \sqrt{K\rho}$ vary in space. In general both will vary, but special choices can be made so that either is constant. Figure 2 shows the typical behavior in each of the four possible types of media: homogeneous (top left); constant Z and variable c (top right); constant c and variable Z (bottom left); and variable c and Z (bottom right). Each medium consists of alternating horizontal layers:

$$K(y), \rho(y) = \begin{cases} (K_A, \rho_A) \text{ if } \left| y - \lfloor y \rfloor - \frac{1}{2} \right| < \frac{1}{4}, \\ (K_B, \rho_B) \text{ if } \left| y - \lfloor y \rfloor - \frac{1}{2} \right| > \frac{1}{4}. \end{cases} \tag{2}$$

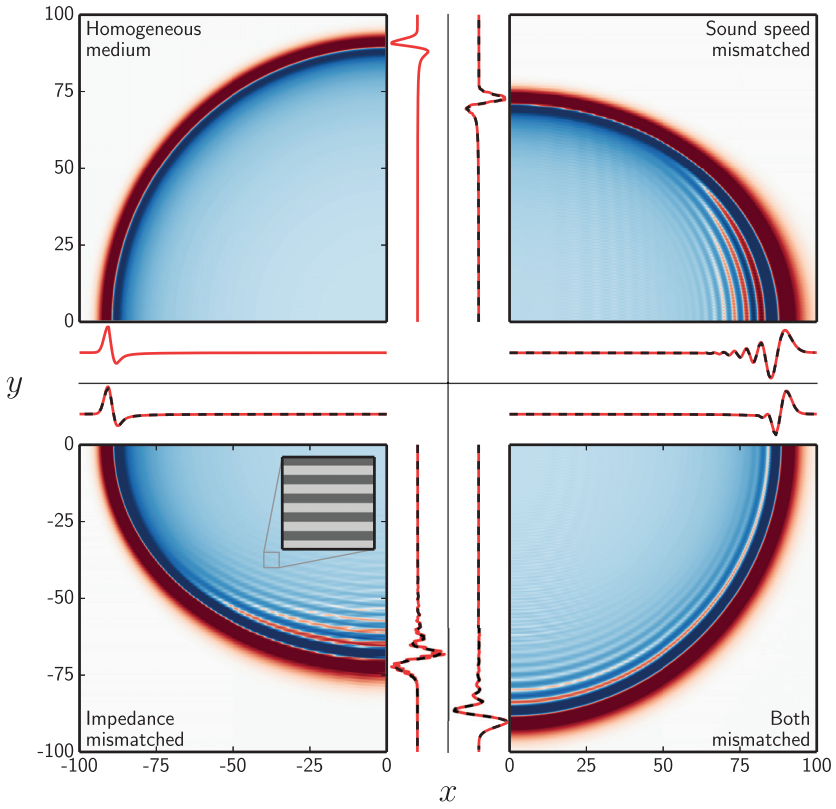

FIG. 2. *Wave propagation in four types of layered periodic media. The units are scaled to the medium period, and the inset shows the layered medium structure. The adjacent line plots show slices of the solution along the lines $x = 0$ (normal) and $y = 0$ (transverse). In the slice plots, the dotted black lines are approximations based on the effective medium equations derived in section 2. Notice how dispersion is evident in the y-direction when the impedance varies (bottom plots) and in the x-direction when the sound speed varies (right plots).*

In each case, the solution shown corresponds to one quadrant of the evolution of an initially Gaussian perturbation:

$$p_0(x, y) = e^{-\frac{x^2+y^2}{2\sigma^2}}, \qquad u_0 = v_0 = 0, \tag{3}$$

with $\sigma = 2$. The line plots show traces of the solution along the lines $x = 0$ (normal) and $y = 0$ (transverse). The solutions are computed using highly resolved finite volume simulations.

Two important effects are evident. First, the speed of wave propagation is *anisotropic* in the heterogeneous media; typically, normally incident waves travel more slowly. This is not surprising, given that such waves undergo partial reflection at each material interface. This effect is explained well by the lowest-order homogenization theory. The second effect is that, depending on the nature of the medium, different components of the wave may develop a dispersive tail. These *dispersive* effects cannot be described by the lowest-order homogenization.

For waves propagating in the normal direction ($\theta = 90°$), we observe that dispersion occurs when the material impedance varies (bottom plots) and not when the impedance is constant (top plots). Indeed, the propagation of a plane wave along

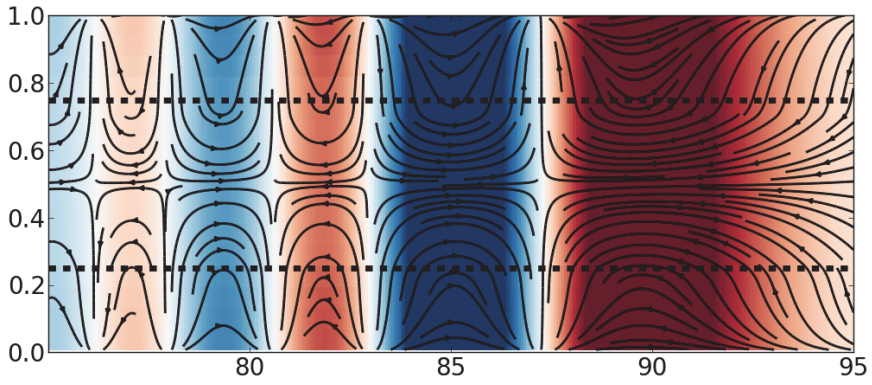

FIG. 3. *Closeup of a transversely propagating part of the solution for the c-dispersive medium from the top right quadrant of Figure 2. Streamlines of the velocity field (in black) superimposed on pressure (in color). The wavefront is propagating to the right, but significant diffraction is present, as indicated by the vertical velocity components. The dashed lines represent the material interfaces.*

the y-axis (normal propagation) reduces to a one-dimensional problem that is well-studied. Over long distances, periodic variation in the material impedance leads to a dispersive effect—higher frequencies travel more slowly, due to reflection [12]. We refer to this as *reflective dispersion*. On the other hand, when the impedance does not vary, there is no reflection and no effective dispersion [12, 10]. Instead, all wavelengths travel at the harmonic average of the sound speed.

Next, let us examine the propagation of waves in the transverse direction ($\theta = 0°$). From the left plots, we see that such waves undergo no dispersion when the material sound speed is constant. Remarkably, the right plots show that transverse waves are dispersed when the sound speed varies. In this work, we show that diffraction can play a role similar to that of reflection in periodic media, leading again to a dispersive effect in which higher frequencies travel more slowly. Thus an effective dispersion arises even in materials with constant impedance. This *diffractive dispersion* is an inherently multidimensional effect with no one-dimensional analogue. Whereas reflective dispersion depends on variation in the material impedance, diffractive dispersion depends on variation in the material sound speed.

In Figure 3, we plot streamlines of the velocity field superimposed on a color plot of the pressure, and the dashed lines represent the material interfaces. The presence of diffraction is evident in the velocity streamlines. It should be noted that the streamlines do not represent particle trajectories; they are merely a helpful tool for visualizing the vertical velocity components created by diffraction.

The dotted black lines in the slice plots are based on pseudospectral solutions of the effective medium equations (32), derived in section 2. (No corresponding line is shown in the top left quadrant, since the "effective medium" is exact in the homogeneous case.) At the resolution shown in the figure, they are indistinguishable from the "exact" finite volume solutions. The agreement between the effective and variable-coefficient equations is explored in section 4.

It has been observed that reflective dispersion can, in combination with nonlinear effects, lead to the formation of solitary waves [10]. Diffractive dispersion can also lead to formation of nonlinear solitary waves; this is the subject of current research [8].

2. Homogenization. Homogenization theory can be used to derive an effective PDE for waves in a periodic medium when the wavelength λ is larger than the period of

the medium Ω. The effective PDE is derived through a perturbation expansion, using $\delta = \Omega/\lambda$ as a small parameter. We will see that the homogenized PDE depends only on Ω and not on λ. Since the effective PDE has constant coefficients, it can be used to determine an effective dispersion relation for plane waves in the periodic medium.

The lowest-order homogenized equation for (1) (containing only terms of $\mathcal{O}(\delta^0)$) is well understood already, but it contains no dispersive terms and so cannot describe even qualitatively the results shown in the introduction. In this section we derive homogenized equations including terms up to $\mathcal{O}(\delta^4)$, which include dispersive terms. Additional terms up to $\mathcal{O}(\delta^6)$ are derived for a plane wave propagating in the x-direction. Our approach is based on the technique used in [3] for one-dimensional wave propagation. We will see that some care is required to extend the technique used there to the case of two-dimensional media of the type shown in Figure 1. We remark that further difficulties arise when considering periodic media in which the coefficients depend on both x and y; we do not pursue high-order homogenization for such materials here.

It will be convenient to deal with the wave equation (1) in first-order form:

$$p_t + K(y)(u_x + v_y) = 0, \tag{4a}$$

$$\rho(y)u_t + p_x = 0, \tag{4b}$$

$$\rho(y)v_t + p_y = 0. \tag{4c}$$

Here u, v are the velocities in the x- and y-coordinate directions, respectively.

We start by introducing a fast scale $\hat{y} = \delta^{-1}y$ and adopting the formalism that y and $\hat{y}$ are independent. The scale defined by $\hat{y}$ is the scale on which the material properties vary, so we formally replace the Ω-periodic functions $K(y), \rho(y)$ with λ-periodic functions $\hat{K}(\hat{y})$ and $\hat{\rho}(\hat{y})$, which are independent of the slow scale y. The dependent variables p, u, v are assumed to vary on both the fast and slow scales and are assumed to be periodic in $\hat{y}$ with period λ. The idea now is to average over the fast scale $\hat{y}$ to obtain constant-coefficient equations involving only y. These equations will not capture the details of the solution on the fast scale but will include (to some degree) the influence of the fast scale on the slow scale.

Using the chain rule we find that $\partial_y \mapsto \partial_y + \delta^{-1}\partial_{\hat{y}}$. Therefore, system (4) becomes

$$\hat{K}^{-1}(\hat{y})p_t + u_x + v_y + \delta^{-1}v_{\hat{y}} = 0, \tag{5a}$$

$$\hat{\rho}(\hat{y})u_t + p_x = 0, \tag{5b}$$

$$\hat{\rho}(\hat{y})v_t + p_y + \delta^{-1}p_{\hat{y}} = 0. \tag{5c}$$

For simplicity, from here on we omit the hats over the coefficient function K and ρ, with the understanding that all material coefficients are λ-periodic functions of $\hat{y}$. Next we assume that p, u, and v can be formally written as power series in δ, e.g., $p(x, y, \hat{y}, t) = \sum_{i=0}^{\infty} \delta^i p_i(x, y, \hat{y}, t)$. Plugging these expansions into (5) yields

$$K^{-1}\sum_{i=0}^{\infty}\delta^i p_{i,t} + \sum_{i=0}^{\infty}\delta^i u_{i,x} + \sum_{i=0}^{\infty}\delta^i v_{i,y} + \delta^{-1}\sum_{i=0}^{\infty}\delta^i v_{i,\hat{y}} = 0, \tag{6a}$$

$$\rho\sum_{i=0}^{\infty}\delta^i u_{i,t} + \sum_{i=0}^{\infty}\delta^i p_{i,x} = 0, \tag{6b}$$

$$\rho\sum_{i=0}^{\infty}\delta^i v_{i,t} + \sum_{i=0}^{\infty}\delta^i p_{i,y} + \delta^{-1}\sum_{i=0}^{\infty}\delta^i p_{i,\hat{y}} = 0, \tag{6c}$$

where $(\cdot)_{i,x}$ denotes differentiation of $(\cdot)_i$ with respect to x. Next we equate terms of the same order in δ; at each order we apply the averaging operator

$$\langle\cdot\rangle := \frac{1}{\lambda}\int_0^\lambda (\cdot)d\hat{y} \tag{7}$$

to obtain the homogenized leading-order system and corrections to it. Thus the homogenized equations don't depend on the fast scale $\hat{y}$. Note that the averaging operator averages over one period in y, i.e., from 0 to Ω; therefore, in $\hat{y}$ it averages from 0 to λ, i.e., since $y = \delta\hat{y} = \frac{\Omega}{\lambda}\hat{y}$, we have

$$\frac{1}{\Omega}\int_0^\Omega (\cdot)dy = \frac{1}{\lambda}\int_0^\lambda (\cdot)d\hat{y}. \tag{8}$$

For brevity in longer equations, we will sometimes use a bar instead of brackets to denote this average (i.e., $\bar{f} = \langle f\rangle$).

We present the derivation of the first two corrections in detail. Since the derivation of higher-order terms is similar (but increasingly tedious), we give the higher-order results without detailed derivations. Most of the process is mechanical, but for each system we must make an intelligent ansatz to obtain an expression for the nonhomogenized solution of the corresponding system.

2.1. Homogenized $\mathcal{O}(1)$ system. Taking only $\mathcal{O}(\delta^{-1})$ terms in (6) gives

$$v_{0,\hat{y}} = 0, \tag{9a}$$

$$p_{0,\hat{y}} = 0, \tag{9b}$$

which implies $v_0 =: \bar{v}_0(x,y,t)$ and $p_0 =: \bar{p}_0(x,y,t)$. Thus the leading-order pressure and vertical velocity are independent of the fast scale $\hat{y}$. Note that we can't assume that u_0 is independent of $\hat{y}$; we will see in the following sections that it is not. This is in contrast to the homogenization of similar systems in one dimension where, to leading order, all dependent variables are independent of the fast scale [3].

Taking only the $\mathcal{O}(1)$ terms in (6) gives

$$K^{-1}\bar{p}_{0,t} + u_{0,x} + \bar{v}_{0,y} + v_{1,\hat{y}} = 0, \tag{10a}$$

$$\rho u_{0,t} + \bar{p}_{0,x} = 0, \tag{10b}$$

$$\rho\bar{v}_{0,t} + \bar{p}_{0,y} + p_{1,\hat{y}} = 0. \tag{10c}$$

Next we apply the averaging operator $\langle\cdot\rangle$ to (10). This eliminates the terms $v_{1,\hat{y}}$ and $p_{1,\hat{y}}$, which are periodic with mean zero. We have no way to determine the average of $\rho u_{0,t}$ because both ρ and u_0 depend on $\hat{y}$. We therefore divide (10b) by ρ and then apply $\langle\cdot\rangle$, yielding

$$K_h^{-1}\bar{p}_{0,t} + \bar{u}_{0,x} + \bar{v}_{0,y} = 0, \tag{11a}$$

$$\rho_h\bar{u}_{0,t} + \bar{p}_{0,x} = 0, \tag{11b}$$

$$\rho_m\bar{v}_{0,t} + \bar{p}_{0,y} = 0, \tag{11c}$$

where here and elsewhere the subscripts m and h denote the arithmetic and harmonic average, respectively:

$$\rho_m := \langle\rho\rangle, \qquad \rho_h := \left\langle\rho^{-1}\right\rangle^{-1},$$

$$K_m := \langle K\rangle, \qquad K_h := \left\langle K^{-1}\right\rangle^{-1}.$$

We see already that the effective medium is anisotropic, as indicated by the appearance of these different averages of ρ in (11b) and (11c). In particular, we see that plane waves propagating parallel to the y-axis travel with speed $\sqrt{\frac{K_h}{\rho_m}}$ while plane waves propagating parallel to the x-axis travel with speed $\sqrt{\frac{K_h}{\rho_h}}$. We discuss this in more detail in section 3.1.

Combining (10b) and (11b) yields

$$u_0 = \frac{\rho_h}{\rho(\hat{y})}\bar{u}_0 + c, \tag{12}$$

where c is a time independent constant. We choose $\bar{u}_0(x, y, t = 0) = \frac{\rho(\hat{y})}{\rho_h} u_0(x, y, \hat{y}, t = 0)$ so that $c = 0$. This confirms that u_0 varies on the fast scale $\hat{y}$. More importantly, this indicates that propagation in x is affected by the heterogeneity in y even at the macroscopic scale.

Next we obtain expressions for u_1, v_1 and p_1 in (10). To do so, we use the following ansatz:

$$v_1 = \bar{v}_1 + A(\hat{y})\bar{u}_{0,x} + B(\hat{y})\bar{v}_{0,y}, \tag{13a}$$

$$p_1 = \bar{p}_1 + C(\hat{y})\bar{p}_{0,y}. \tag{13b}$$

This ansatz is chosen in order to reduce system (10) to a system of ODEs. Substituting the ansatz (13), the relation (12), and the homogenized leading-order system (11) into the the $\mathcal{O}(1)$ system (10), we get

$$(A_{\hat{y}} - K_h K^{-1} + \rho_h \rho^{-1})\bar{u}_{0,x} + (B_{\hat{y}} - K_h K^{-1} + 1)\bar{v}_{0,x} = 0, \tag{14}$$

$$(C_{\hat{y}} - \rho\rho_m^{-1} + 1)\bar{p}_{0,y} = 0. \tag{15}$$

Based on this, it is convenient to choose $A(\hat{y})$, $B(\hat{y})$, and $C(\hat{y})$ to satisfy

$$A_{\hat{y}} - K^{-1}K_h + \rho^{-1}\rho_h = 0, \tag{16a}$$

$$B_{\hat{y}} - K^{-1}K_h - 1 = 0, \tag{16b}$$

$$C_{\hat{y}} - \rho\rho_m^{-1} + 1 = 0. \tag{16c}$$

Equations (16) represent boundary value ODEs with the normalization conditions that $\langle A\rangle = \langle B\rangle = \langle C\rangle = 0$. Note that $\langle A_{\hat{y}}\rangle = \langle B_{\hat{y}}\rangle = \langle C_{\hat{y}}\rangle = 0$, which implies that A, B, and C are λ-periodic. To solve these boundary value problems we must specify the material functions ρ, K. In Appendix A we show the fast-variable functions A, B, and C for a layered medium. It is convenient to introduce the following linear operators (see [10, p. 1554]):

$$\{a\}(\hat{y}) = a(\hat{y}) - \langle a(\hat{y})\rangle, \tag{17a}$$

$$[\![a]\!](\hat{y}) = \int_s^{\hat{y}} \{a\}(\xi)d\xi, \qquad \text{where } s \text{ is chosen such that } \langle [\![a\rangle\,(\hat{y})]\!] = 0. \tag{17b}$$

Then we have

$$A = [\![K^{-1}K_h - \rho^{-1}\rho_h]\!], \tag{18a}$$

$$B = [\![K^{-1}K_h]\!], \tag{18b}$$

$$C = [\![\rho\rho_m^{-1}]\!]. \tag{18c}$$

2.2. Derivation of $\mathcal{O}(\delta)$ system. Taking only the $\mathcal{O}(\delta)$ terms in (6) gives

$$K^{-1}p_{1,t} + u_{1,x} + v_{1,y} + v_{2,\hat{y}} = 0, \tag{19a}$$

$$\rho u_{1,t} + p_{1,x} = 0, \tag{19b}$$

$$\rho v_{1,t} + p_{1,y} + p_{2,\hat{y}} = 0. \tag{19c}$$

Substituting the ansatz for v_1 and p_1 from (13) into (19) and averaging gives

$$K_h^{-1}\bar{p}_{1,t} + \bar{u}_{1,x} + \bar{v}_{1,y} = -\left\langle K^{-1}C\right\rangle \bar{p}_{0,yt}, \tag{20a}$$

$$\rho_h \bar{u}_{1,t} + \bar{p}_{1,x} = -\rho_h \left\langle \rho^{-1}C\right\rangle \bar{p}_{0,xy}, \tag{20b}$$

$$\rho_m \bar{v}_{1,t} + \bar{p}_{1,y} = -\left\langle \rho A\right\rangle \bar{u}_{0,xt} - \left\langle \rho B\right\rangle \bar{v}_{0,yt}, \tag{20c}$$

where $\bar{u}_1 := \langle u_1\rangle$ and similarly for $\bar{v}_1$ and $\bar{p}_1$. For any piecewise-constant functions f, g it can be shown that $\langle f[\![g]\!]\rangle = 0$ [10]. Thus, for the piecewise-constant materials that we consider in section 4, we have $\left\langle K^{-1}C\right\rangle = \left\langle \rho^{-1}C\right\rangle = \langle \rho A\rangle = \langle \rho B\rangle = 0$. These averages also vanish for the sinusoidal materials we will consider. For more general materials, these terms may be nonzero, but in the following we assume they vanish. Then we obtain

$$K_h^{-1}\bar{p}_{1,t} + \bar{u}_{1,x} + \bar{v}_{1,y} = 0, \tag{21a}$$

$$\rho_h \bar{u}_{1,t} + \bar{p}_{1,x} = 0, \tag{21b}$$

$$\rho_m \bar{v}_{1,t} + \bar{p}_{1,y} = 0. \tag{21c}$$

Since the boundary conditions are imposed in the leading-order homogenized system (11), system (21) should be solved with homogeneous Dirichlet boundary conditions; therefore, its solution vanishes:

$$\bar{u}_1 = \bar{v}_1 = \bar{p}_1 = 0. \tag{22}$$

Taking $\bar{u}_1 = \bar{v}_1 = \bar{p}_1 = 0$, we make the following ansatz for the $\mathcal{O}(\delta)$ solutions v_2 and p_2,

$$\begin{aligned} v_2 &= \bar{v}_2 + D(\hat{y})\bar{u}_{0,xy} + E(\hat{y})\bar{v}_{0,yy}, \\ p_2 &= \bar{p}_2 + F(\hat{y})\bar{p}_{0,yy} + H(\hat{y})\bar{p}_{0,xx}, \end{aligned} \tag{23}$$

which is chosen in order to reduce system (19) to a system of ODEs. From (19b) we get $u_{1,t} = -\rho^{-1}p_{1,x}$. The ansatz for p_1 from (13b) gives $u_{1,t} = -\rho^{-1}C(\bar{p}_{0,x})_y$, and using the homogenized leading-order equation (11b) we get $u_{1,t} = \rho^{-1}\rho_h C(\bar{u}_{0,y})_t$. Finally, we get an expression for the nonhomogenized solution u_1:

$$u_1 = \rho^{-1}\rho_h C\bar{u}_{0,y}. \tag{24}$$

Next we substitute the ansatz for v_1 and p_1 from (13), the ansatz for v_2 and p_2 from (23), and the nonhomogenized solution u_1 from (24) into system (19). Then we substitute the leading-order homogenized system (11) and the coefficients (18a). Finally, in the resulting expression, we make the fast-variable coefficients to vanish to obtain

$$D = [\![K^{-1}K_h C - \rho^{-1}\rho_h C - A]\!], \tag{25a}$$

$$E = [\![K^{-1}K_h C - B]\!], \tag{25b}$$

$$F = [\![\rho\rho_m^{-1}B - C]\!], \tag{25c}$$

$$H = [\![\rho\rho_h^{-1}A]\!]. \tag{25d}$$

2.3. Derivation of $\mathcal{O}(\delta^2)$ system. From (6) we take $\mathcal{O}(\delta^2)$ terms to get

$$K^{-1}p_{2,t} + u_{2,x} + v_{2,y} + v_{3,\hat{y}} = 0, \tag{26a}$$

$$\rho u_{2,t} + p_{2,x} = 0, \tag{26b}$$

$$\rho v_{2,t} + p_{2,y} + p_{3,\hat{y}} = 0. \tag{26c}$$

Substituting the ansatz for v_2 and p_2 from (23) into (26) and averaging yields

$$K_h^{-1}\bar{p}_{2,t} + \bar{u}_{2,x} + \bar{v}_{2,y} = \alpha_1(\bar{u}_{0,xyy} + \bar{v}_{0,yyy}) + \alpha_2(\bar{u}_{0,xxx} + \bar{v}_{0,xxy}), \tag{27a}$$

$$\rho_h\bar{u}_{2,t} + \bar{p}_{2,x} = \beta_1\bar{p}_{0,xyy} + \beta_2\bar{p}_{0,xxx}, \tag{27b}$$

$$\rho_m\bar{v}_{2,t} + \bar{p}_{2,y} = \gamma_1\bar{p}_{0,yyy} + \gamma_2\bar{p}_{0,xxy}, \tag{27c}$$

where $\bar{u}_2 := \langle u_2 \rangle$ and similarly for $\bar{v}_2$ and $\bar{p}_2$. Expressions for the coefficients α, β, γ appear in Appendix B.

2.4. Higher-order corrections. Following similar, but more involved steps, we find the $\mathcal{O}(\delta^3)$ and $\mathcal{O}(\delta^4)$ corrections.

2.4.1. $\mathcal{O}(\delta^3)$ homogenized correction. The third homogenized correction is

$$K_h^{-1}\bar{p}_{3,t} + \bar{u}_{3,x} + \bar{v}_{3,y} = -\left\langle K^{-1}C\right\rangle \bar{p}_{2,yt} - \left\langle K^{-1}N\right\rangle \bar{p}_{0,yyyt} - \left\langle K^{-1}P\right\rangle \bar{p}_{0,xxyt}, \tag{28a}$$

$$\rho_h\bar{u}_{3,t} + \bar{p}_{3,x} = -\rho_h\left\langle \rho^{-1}C\right\rangle \bar{p}_{2,xy} - \rho_h\left\langle \rho^{-1}N\right\rangle \bar{p}_{0,xyyy} - \rho_h\left\langle \rho^{-1}P\right\rangle \bar{p}_{0,xxxy}, \tag{28b}$$

$$\begin{aligned}\rho_m\bar{v}_{3,t} + \bar{p}_{3,y} = &-\langle \rho A\rangle\, \bar{u}_{2,xt} - \langle \rho B\rangle\, \bar{v}_{2,yt} \\ &- \langle \rho I\rangle\, \bar{u}_{0,xyyt} - \langle \rho J\rangle\, \bar{u}_{0,xxxt} - \langle \rho L\rangle\, \bar{v}_{0,xxyt} - \langle \rho M\rangle\, \bar{v}_{0,yyyt},\end{aligned} \tag{28c}$$

where $\bar{u}_3 := \langle u_3 \rangle$ and similarly for $\bar{v}_3$ and $\bar{p}_3$. The fast-variable functions $I(\hat{y})$, $J(\hat{y})$, $L(\hat{y})$, $M(\hat{y})$, $N(\hat{y})$, $P(\hat{y})$ are solutions of the BVPs

$$I = [\![K^{-1}K_h\left(F - K_h\left\langle K^{-1}F\right\rangle\right) - \rho^{-1}\rho_h\left(F - \rho_h\left\langle \rho^{-1}F\right\rangle\right) - D]\!], \tag{29a}$$

$$J = [\![K^{-1}K_h\left(H - K_h\left\langle K^{-1}H\right\rangle\right) - \rho^{-1}\rho_h\left(H - \rho_h\left\langle \rho^{-1}H\right\rangle\right)]\!], \tag{29b}$$

$$L = [\![K^{-1}K_h\left(H - K_h\left\langle K^{-1}H\right\rangle\right)]\!], \tag{29c}$$

$$M = [\![K^{-1}K_h\left(F - K_h\left\langle K^{-1}F\right\rangle\right) - E]\!], \tag{29d}$$

$$N = [\![\rho\rho_m^{-1}\left(E - \rho_m^{-1}\left\langle \rho E\right\rangle\right) - F]\!], \tag{29e}$$

$$P = [\![\rho\rho_h^{-1}\left(D - \rho_m^{-1}\left\langle \rho D\right\rangle\right) - H]\!]. \tag{29f}$$

For the two types of media considered in this work, all coefficients on the right-hand side of (28) vanish. Since the boundary conditions are fulfilled by the leading-order homogenized system (11), the third homogenized correction vanishes, i.e.,

$$\bar{u}_3 = \bar{v}_3 = \bar{p}_3 = 0. \tag{30}$$

2.4.2. $\mathcal{O}(\delta^4)$ homogenized correction. The fourth correction is given by

$$\begin{aligned}K_h^{-1}\bar{p}_{4,t} + \bar{u}_{4,x} + \bar{v}_{4,y} = &\alpha_1(\bar{u}_{2,xyy} + \bar{v}_{2,yyy}) + \alpha_2(\bar{u}_{2,xxx} + \bar{v}_{2,xxy}) \\ &+ \alpha_3(\bar{u}_{0,xyyyy} + \bar{v}_{0,yyyyy}) + \alpha_4(\bar{u}_{0,xxxxx} + \bar{v}_{0,xxxxy}) \\ &+ \alpha_5(\bar{u}_{0,xxxyy} + \bar{v}_{0,xxyyy}),\end{aligned} \tag{31a}$$

$$\begin{aligned}\rho_h\bar{u}_{4,t} + \bar{p}_{4,x} = &\beta_1\bar{p}_{2,xyy} + \beta_2\bar{p}_{2,xxx} \\ &+ \beta_3\bar{p}_{0,xyyyy} + \beta_4\bar{p}_{0,xxxxx} + \beta_5\bar{p}_{0,xxxyy},\end{aligned} \tag{31b}$$

$$\begin{aligned}\rho_m\bar{v}_{4,t} + \bar{p}_{4,y} = &\gamma_1\bar{p}_{2,yyy} + \gamma_2\bar{p}_{2,xxy} \\ &+ \gamma_3\bar{p}_{0,yyyyy} + \gamma_4\bar{p}_{0,xxyyy} + \gamma_5\bar{p}_{0,xxxxy},\end{aligned} \tag{31c}$$

where $\bar{u}_4 := \langle u_4 \rangle$ and similarly for $\bar{v}_4$ and $\bar{p}_4$. Expressions for the coefficients α, β, γ are given in Appendix B

2.5. Combined homogenized equations. Once we have the homogenized leading-order system and the homogenized corrections, we can combine them into a single system. This is done by taking $\bar{p} := \langle p_0 + \delta p_1 + \cdots + \delta^4 p_4 \rangle = \bar{p}_0 + \delta \bar{p}_1 + \cdots + \delta^4 \bar{p}_4$ and similarly for $\bar{u}$ and $\bar{v}$. Combining homogenized systems (11), (21), (27), (28), and (31), we obtain

$$\begin{aligned} K_h^{-1}\bar{p}_t + \bar{u}_x + \bar{v}_y &= \delta^2 \left[\alpha_1(\bar{u}_{xyy} + \bar{v}_{yyy}) + \alpha_2(\bar{u}_{xxx} + \bar{v}_{xxy})\right] \\ &\quad + \delta^4 \left[\alpha_3(\bar{u}_{xyyyy} + \bar{v}_{yyyyy}) + \alpha_4(\bar{u}_{xxxxx} + \bar{v}_{xxxxy})\right] \\ &\quad + \delta^4 \left[\alpha_5(\bar{u}_{xxxyy} + \bar{v}_{xxyyy})\right], \end{aligned} \tag{32a}$$

$$\rho_h \bar{u}_t + \bar{p}_x = \delta^2 \left[\beta_1 \bar{p}_{xyy} + \beta_2 \bar{p}_{xxx}\right] + \delta^4 \left[\beta_3 \bar{p}_{xyyyy} + \beta_4 \bar{p}_{xxxxx} + \beta_5 \bar{p}_{xxxyy}\right], \tag{32b}$$

$$\rho_m \bar{v}_t + \bar{p}_y = \delta^2 \left[\gamma_1 \bar{p}_{yyy} + \gamma_2 \bar{p}_{xxy}\right] + \delta^4 \left[\gamma_3 \bar{p}_{yyyyy} + \gamma_4 \bar{p}_{xxyyy} + \gamma_5 \bar{p}_{xxxxy}\right], \tag{32c}$$

where expressions for the coefficients are given in Appendix B. Unlike the lowest-order homogenized equation (10), this system is dispersive and the dispersion depends on the direction of propagation; see section 3.

In general, each coefficient of a $\delta^n = \frac{\Omega^n}{\lambda^n}$ term in (32) contains a matching factor λ^n (contained within the $\alpha's$ and $\beta's$; see Appendix B.1 for an example of the coefficients of the first-order solution for a layered medium). As a result, each term on the right-hand side of (32) is proportional to Ω^n (and independent of λ). This explains the observation in [10] that the homogenized equations are valid for any choice of the material period Ω. Nevertheless, (32) is only valid for small δ, i.e., for relatively long wavelengths $\lambda > \Omega$. In all numerical simulations in this work, we take $\Omega = 1$.

3. Effective dispersion relations. Equation (32) is a linear system of PDEs with constant coefficients. Hence, its solutions can be completely described by the dispersion relation, which relates frequency and wavenumber for a plane wave:

$$\bar{p}(x, y, t) = \bar{p}_0 e^{i(\mathbf{k}\cdot\mathbf{x} - \omega t)}. \tag{33}$$

Here $\bar{p}_0$ is the amplitude, ω is the angular frequency, and $\mathbf{k}$ is the wave vector. Let $\mathbf{k} = k(k_x, k_y)$ with $k_x = \cos\theta, k_y = \sin\theta$, where θ is the direction of propagation (see Figure 1). Because (32) describes a medium that is anisotropic and dispersive, the speed of propagation of a plane wave depends on both the angle θ and the wavenumber magnitude k.

We can combine (32) into a single second-order equation by differentiating (32a) with respect to t, differentiating (32b) and (32c) with respect to x and y, respectively, and equating mixed partial derivatives. By substituting (33) into the result, we obtain the effective dispersion relation, up to $\mathcal{O}(\delta^4)$:

$$\begin{aligned} \omega^2 = {} & \frac{K_h}{\rho_h \rho_m} k^2 \left(k_x^2 \rho_m + k_y^2 \rho_h\right) + \delta^2 \frac{K_h}{\rho_h \rho_m} k^4 \left[k_x^2 \rho_m \left(\left(\alpha_2 + \beta_2\right) k_x^2 + \left(\alpha_1 + \beta_1\right) k_y^2\right)\right. \\ & \left. + k_y^2 \rho_h \left(\left(\alpha_2 + \gamma_2\right) k_x^2 + \left(\alpha_1 + \gamma_1\right) k_y^2\right)\right] \\ & + \delta^4 \frac{K_h}{\rho_h \rho_m} k^6 [k_x^2 \rho_m \left(\left(\alpha_4 + \alpha_2\beta_2 - \beta_4\right) k_x^4 - \left(\alpha_5 - \alpha_2\beta_1 - \alpha_1\beta_2 + \beta_5\right) k_x^2 k_y^2\right. \\ & \left. + \left(\alpha_3 + \alpha_1\beta_1 - \beta_3\right) k_y^4\right) \\ & + k_y^2 \rho_h \left(\left(\alpha_4 + \alpha_2\gamma_2 - \gamma_5\right) k_x^4 - \left(\alpha_5 - \alpha_2\gamma_1 - \alpha_1\gamma_2 + \gamma_4\right) k_x^2 k_y^2\right. \\ & \left. + \left(\alpha_3 + \alpha_1\gamma_1 - \gamma_3\right) k_y^4\right)]. \end{aligned} \tag{34}$$

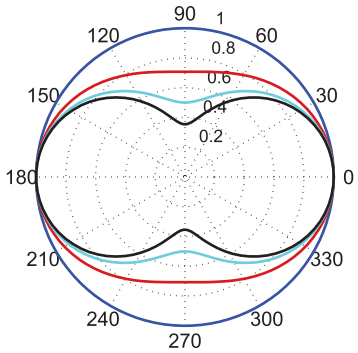

FIG. 4. *Polar plot of the effective sound speed* (35) *with* $K_h = 1$, $\rho_h = 1$, *and* $\rho_m = 1$ *(blue),* $\rho_m = 2$ *(red),* $\rho_m = 4$ *(cyan),* $\rho_m = 8$ *(black).*

It is important to keep in mind that although (34) is accurate to $\mathcal{O}(\delta^4)$, it is obtained by homogenization and is not expected to be valid for wavelengths shorter than Ω, the medium period. This is because $\delta = \frac{\Omega}{\lambda}$ is assumed to be small; in particular, $\delta < 1$.

3.1. Effective sound speed. Taking only $\mathcal{O}(1)$ terms in (34), we obtain the effective sound speed:

$$c_{\text{eff}} = \omega/k = \sqrt{\frac{K_h}{\rho_h}k_x^2 + \frac{K_h}{\rho_m}k_y^2}. \tag{35}$$

The effective sound speed, which indicates the speed of very long wavelength perturbations, depends on the direction of propagation. For normally incident waves ($\theta = 90°$), we have $c_{\text{eff}} = \sqrt{K_h/\rho_m}$, which is the effective sound speed in a one-dimensional layered medium [12]. For transverse waves ($\theta = 0°$), we have $c_{\text{eff}} = \sqrt{K_h/\rho_h}$. Since the harmonic average is less than or equal to the arithmetic average, long-wavelength normal waves never travel faster than their transverse wave counterparts. This is intuitively reasonable since transverse propagating waves undergo no reflection.

In Figure 4 we plot c_{eff} as a function of θ for material parameters $K_h = 1$, $\rho_h = 1$ and different values of ρ_m. When $\rho_h = \rho_m$, the sound speed is the same in all directions so we obtain the blue line in Figure 4. As ρ_m increases (corresponding to strong impedance variation and thus more reflection), the effective speed in y decreases and we obtain the red, cyan, and black lines in Figure 4. In Figure 5 we take the initial condition

$$\bar{p}_0(x,y) = 5e^{-\frac{(x-20)^2+(y-10)^2}{2\sigma^2}}, \qquad \bar{u}_0 = \bar{v}_0 = 0, \tag{36}$$

with $\sigma^2 = 10$ and a piecewise-constant medium (2) with $\rho_A = 8 + \sqrt{56}$, $\rho_B = 8/\rho_A$, and $K_A = K_B = 1$, which gives $K_h = \rho_h = 1$ and $\rho_m = 8$, corresponding to the black line in Figure 4. We show the homogenized leading-order pressure (left) and the finite volume pressure (right) at $t = 5$, which correspond to the solutions of (11) and (1), respectively. The predicted anisotropic behavior is observed in both solutions.

3.2. Normally and transversely incident waves. The dispersion relation (34) has some special properties for waves that are aligned with the coordinate axes.

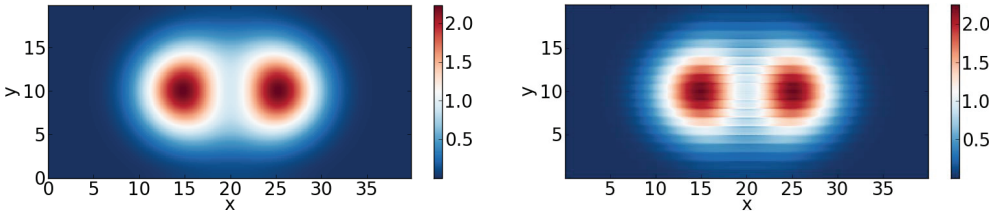

FIG. 5. *Homogenized leading-order solution $\bar{p}$ (left) and finite volume solution p (right) at $t = 5$ in a layered medium with $\rho_A = 8 + \sqrt{56}$, $\rho_B = 8/\rho_A$, and $K_A = K_B = 1$ (which gives $K_h = \rho_h = 1$ and $\rho_m = 8$). This corresponds to the effective sound speed distribution shown in Figure 4 (black line). Note that the horizontal lines in the right figure are the effect of the medium structure and not of numerical resolution (which is much finer).*

Recall the definitions of normal and transverse wave propagation illustrated in Figure 1.

A normally incident plane wave corresponds to initial data that is constant in x. For such waves, (32) reduces to a one-dimensional equation:

$$K_h^{-1}\bar{p}_t + \bar{v}_y = \delta^2\alpha_1\bar{v}_{yyy} + \delta^4\alpha_3\bar{v}_{yyyyy}, \tag{37a}$$

$$\rho_m\bar{v}_t + \bar{p}_y = \delta^2\gamma_1\bar{p}_{yyy} + \delta^4\gamma_3\bar{p}_{yyyyy}. \tag{37b}$$

This system was obtained previously in [12, 3, 10]. For a piecewise-constant medium, the coefficients on the right-hand side are all proportional to the difference of squared impedance, for instance,

$$\alpha_1 = -\left(Z_A^2 - Z_B^2\right)\frac{(K_A - K_B)}{192K_m^2\rho_m}\lambda^2, \tag{38}$$

where $Z_A = \sqrt{K_A\rho_A}$ and $Z_A = \sqrt{K_B\rho_B}$.

In general all of the dispersive terms in (37) vanish when the impedance is constant (see Appendix B). This is because no reflection occurs in such media. This explains why the normally propagating waves in Figure 2 are dispersed in the lower two plots (with variable Z) but not in the upper two plots (with constant Z).

Transversely incident plane waves correspond to initial data that is constant in y. For such waves, (32) simplifies to

$$K_h^{-1}\bar{p}_t + \bar{u}_x = \delta^2\alpha_2\bar{u}_{xxx} + \delta^4\alpha_4\bar{u}_{xxxxx} + \delta^6\alpha_6\bar{u}_{xxxxxxx}, \tag{39a}$$

$$\rho_h\bar{u}_t + \bar{p}_x = \delta^2\beta_2\bar{p}_{xxx} + \delta^4\beta_4\bar{p}_{xxxxx} + \delta^6\beta_6\bar{p}_{xxxxxxx}. \tag{39b}$$

Here we have included additional sixth-order corrections, because this case will be of particular interest in what follows. For a piecewise-constant medium, all coefficients on the right-hand side are proportional to the difference of squared sound speeds, for instance,

$$\alpha_2 = -\left(c_A^2 - c_B^2\right)\frac{(K_A - K_B)}{192K_m^2\rho_m^{-1}}\lambda^2, \tag{40}$$

where $c_A = \sqrt{\frac{K_A}{\rho_A}}$ and $c_B = \sqrt{\frac{K_B}{\rho_B}}$.

In general, all of the dispersive terms in (39) vanish when the sound speed is constant (see Appendix B). This is because no diffraction occurs for transversely incident plane waves in such media. This explains why the transversely propagating

waves in Figure 2 are dispersed in the right two plots (with variable c) but not in the left two plots (with constant c).

Thus we see that, with respect to dispersion, the role played by impedance for normal wave propagation corresponds to the role played by sound speed for transverse wave propagation, and vice versa.

4. Comparison of effective medium and variable-coefficient medium solutions. In this section, we compare in greater detail the solutions obtained from the homogenized effective medium equations (32) and from the variable-coefficient equation (1). Solutions of the homogenized equations are obtained using a Fourier spectral collocation method in space and fourth order Runge–Kutta integration in time [13]. Solutions of the variable-coefficient problem are obtained using PyClaw [6], including numerical methods described in [9, 7, 11]. The code used to produce these results is available from http://github.com/ketch/effective_dispersion_RR.

4.1. Propagation of a plane-wave perturbation. In this section we show the effect of c-dispersion on an initial perturbation that varies only in x:

$$\bar{p}_0(x,y) = 10e^{-\frac{x^2}{10}}, \qquad \bar{u}_0 = \bar{v}_0 = 0.$$

The homogenized equations used are given by (39). To demonstrate that the homogenized equations are valid for more general media, we consider both the piecewise-constant medium (2) and a smoothly varying medium

$$K(y) = \frac{K_A + K_B}{2} + \frac{K_A - K_B}{2}\sin(2\pi y), \tag{41a}$$

$$\rho(y) = \frac{1}{K(y)} \tag{41b}$$

with the material parameters

$$K_A = \frac{1}{\rho_A} = 5/8, \qquad K_B = \frac{1}{\rho_B} = 5/2. \tag{42}$$

For the sinusoidally varying medium we numerically solve the BVPs defining the homogenization coefficients. Mathematica and MATLAB files to solve for these expressions can be found at http://github.com/ketch/effective_dispersion_RR.

Figure 6 shows the results for the two media, after the initial pulse has traveled a distance of more than 1000 material layers. Homogenized solutions of differing orders are shown to demonstrate the increasing accuracy of the high-order homogenized approximations. These results are compared with the finite volume solution of the variable-coefficient wave equation (1), which is averaged in the y-direction (since the homogenized solution represents this average). The agreement is very good, and close examination of the dispersive tail shows that the approximations are increasingly accurate.

4.2. Two-dimensional propagation. We now revisit the result shown in the lower-right quadrant of Figure 2. This involves the propagation of an initially Gaussian pressure perturbation (3) in a piecewise-constant medium (2) with

$$K_A = 17/2, \qquad K_B = 17/32, \qquad \rho_A = \rho_B = 1. \tag{43}$$

In Figure 7(a), we show again the slices along the lines $x = 0$ and $y = 0$, with solid lines indicating the variable-coefficient equation solution and dashed lines indicating

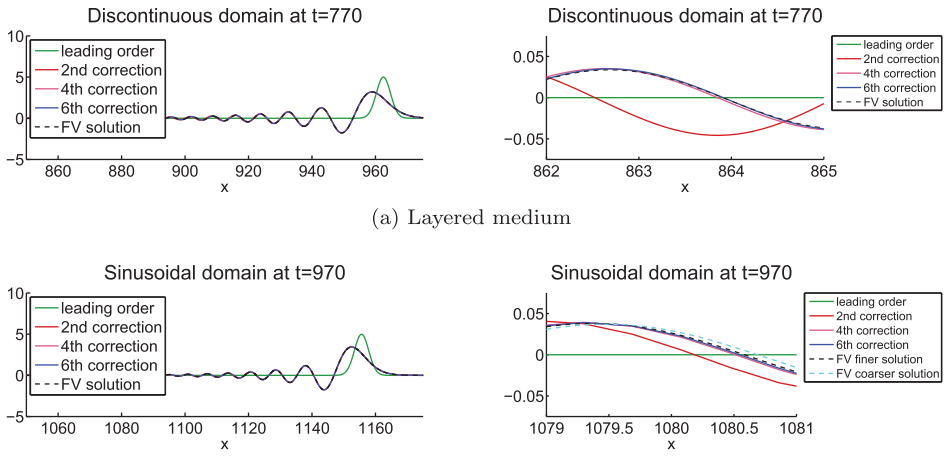

(a) Layered medium

(b) Sinusoidal medium

FIG. 6. *Pressure from homogenized equations with different order corrections versus y-averaged finite volume solution for* (a) *piecewise-constant and* (b) *sinusoidal media. On the right we show a close-up of the dispersive tail where the differences in the homogenized corrections are more noticeable.*

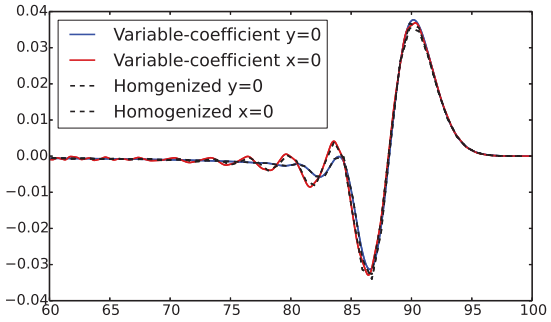

(a) Slices of the solution along the x- (solid blue) and y-axis (solid red). Dashed lines represent slices of the homogenized solution.

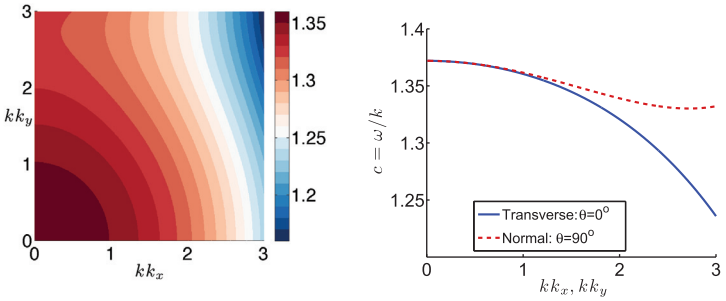

(b) Dispersion relation for this "almost-isotropic" medium. Speed $c = \omega(\mathbf{k})/\mathbf{k}$ is plotted versus wavenumber. The right plot shows slices along $k_x = 0$ and $k_y = 0$.

FIG. 7. *Two-dimensional wave propagation in a piecewise-constant medium with variable Z and c. We show slices along the x- (solid blue) and y-axis (solid red). We also show slices of the homogenized solution (dashed lines).*

the homogenized equations solution. Close agreement between the different approximations is evident.

Furthermore, the leading parts of the wave in the two slices are nearly identical—in other words, even though two very different and direction-dependent dispersive effects are present, the medium behaves almost isotropically. This is the result of a special property of the chosen parameters (43). Due to the approximate symmetry between Z- and c-variation pointed out in section 3.2, it is possible to make the dispersion relation isotropic up to $\mathcal{O}(\delta^2)$ by setting $Z_A = c_A$ and $Z_B = c_B$. The parameters (43) satisfy these conditions. Figure 7(b) shows the dispersion relation for this medium.

5. Discussion. Propagation of long-wavelength waves in periodic media is known to lead to dispersive behavior, usually resulting from small-scale reflection [12]. In this work, we have shown that macroscopic dispersion can also arise due to microscopic diffraction, based on spatial variation of the sound speed. We have focused on media that vary periodically in one direction and are homogeneous in the other. By applying homogenization techniques with carefully chosen assumptions about which variables depend on the small scale, we have obtained a high-order accurate effective medium approximation. Pseudospectral solutions of the effective medium equations agree very well with finite volume solutions of the original variable-coefficient wave equation, even after long times. The homogenized equations can be used to understand the effective dispersion relation of the medium, which depends strongly on the angle of propagation relative to the axis of variation of the medium. By controlling the contrast in impedance and sound speed, it is possible to independently vary the strength of dispersion in the two coordinate directions. Interesting behaviors can be obtained by manipulating these contrasts, for instance, we have shown that certain layered media with variable impedance and sound speed are nevertheless effectively isotropic, up to second order.

It would be interesting to extend this study to media with periodic variation in both x and y. The homogenization process becomes much more challenging in this case, not only because there are more terms, but because it seems that different assumptions are necessary regarding variation on the fast scale. We are also interested in applying our approach to nonlinear systems. This has been done in [8] for a relatively simple system. Extension to the shallow water equations over periodic bathymetry is the subject of ongoing work.

The homogenization carried out here is purely formal. It would be worthwhile to establish precise convergence results and error bounds. This seems to be possible with existing techniques.

We conclude with a particularly interesting observation for which we have not yet found a satisfactory explanation. As pointed out in section 3.2, impedance and sound speed variations seem to play almost dual roles with respect to normal and transverse wave propagation. Equations (37) for normal propagation can be combined to yield the dispersive approximation

$$K_h^{-1}\rho_m\bar{p}_{tt} - \bar{p}_{yy} = \delta^2(\alpha_1 + \gamma_1)\bar{p}_{xxxx} + \mathcal{O}(\delta^4),$$

where for the piecewise-constant medium (2) the leading dispersive term coefficient is

$$\alpha_1 + \gamma_1 = \frac{\left(Z_A^2 - Z_B^2\right)^2}{192K_m^2\rho_m^2}\lambda^2.$$

Meanwhile, equations (39) for transverse propagation can be combined to yield

$$K_h^{-1}\rho_h\bar{p}_{tt} - \bar{p}_{yy} = \delta^2(\alpha_2 + \beta_2)\bar{p}_{xxxx} + \mathcal{O}(\delta^4),$$

where for the piecewise-constant medium (2) the leading dispersive term coefficient is

$$\alpha_2 + \beta_2 = \frac{\left(c_A^2 - c_B^2\right)^2}{192K_m^2}\rho_m\rho_h\lambda^2.$$

The similarity is striking. It is also striking that all dispersive coefficients in the homogenized equations for normal propagation vanish when Z is constant, while all dispersive coefficients in the homogenized equations for transverse propagation vanish when c is constant. We have not tried to prove that this holds in general, but it is true for all media that we have investigated.

Appendix A. Fast-variable functions. In this appendix we show the solution of the fast-variable functions A, B, and C for the layered medium. They are given by

$$A(\hat{y}) = \begin{cases} \frac{\rho_h(c_A^2-c_B^2)(\lambda-4\hat{y})}{8K_m} & \text{if } 0 \le \hat{y} \le 1/2\lambda, \\ \frac{\rho_h(c_B^2-c_A^2)(3\lambda-4\hat{y})}{8K_m} & \text{if } 1/2\lambda \le \hat{y} \le \lambda, \end{cases} \tag{44a}$$

$$B(\hat{y}) = \begin{cases} \frac{(K_A-K_B)(\lambda-4\hat{y})}{8K_m} & \text{if } 0 \le \hat{y} \le 1/2\lambda, \\ -\frac{(K_A-K_B)(3\lambda-4\hat{y})}{8K_m} & \text{if } 1/2\lambda \le \hat{y} \le \lambda, \end{cases} \tag{44b}$$

$$C(\hat{y}) = \begin{cases} -\frac{(\rho_A-\rho_B)(\lambda-4\hat{y})}{8\rho_m} & \text{if } 0 \le \hat{y} \le 1/2\lambda, \\ \frac{(\rho_A-\rho_B)(3\lambda-4\hat{y})}{8\rho_m} & \text{if } 1/2\lambda \le \hat{y} \le \lambda. \end{cases} \tag{44c}$$

The rest of the fast-variable functions are too cumbersome to show here. For the sinusoidal medium, we don't have closed form expressions; instead, we compute the coefficients of the homogenized equations numerically; see Appendix B.2.

Appendix B. Coefficients of homogenized equations. In this appendix we give the coefficients of the homogenized systems (32), (39), and (37). They are

$$\begin{aligned}
\alpha_1 &= K_h\left\langle K^{-1}F\right\rangle, \\
\alpha_2 &= K_h\left\langle K^{-1}H\right\rangle, \\
\alpha_3 &= K_h\left\langle K^{-1}U\right\rangle - K_h^2\left\langle K^{-1}F\right\rangle^2, \\
\alpha_4 &= K_h\left\langle K^{-1}W\right\rangle - K_h^2\left\langle K^{-1}H\right\rangle^2, \\
\alpha_5 &= K_h\left\langle K^{-1}V\right\rangle - 2K_h^2\left\langle K^{-1}F\right\rangle\left\langle K^{-1}H\right\rangle, \\
\alpha_6 &= K_h\left\langle K^{-1}\tilde{B}\right\rangle + K_h^3\left\langle K^{-1}H\right\rangle^3 - 2K_h^2\left\langle K^{-1}H\right\rangle\left\langle K^{-1}W\right\rangle,
\end{aligned}$$

$$\begin{aligned}
\beta_1 &= -\rho_h\left\langle \rho^{-1}F\right\rangle, & \beta_2 &= -\rho_h\left\langle \rho^{-1}H\right\rangle, \\
\beta_3 &= -\rho_h\left\langle \rho^{-1}U\right\rangle, & \beta_4 &= -\rho_h\left\langle \rho^{-1}W\right\rangle, \\
\beta_5 &= -\rho_h\left\langle \rho^{-1}V\right\rangle, & \beta_6 &= -\rho_h\left\langle \rho^{-1}\tilde{B}\right\rangle
\end{aligned}$$

and

$$\begin{aligned}
\gamma_1 &= \rho_m^{-1}\left\langle \rho E\right\rangle, \\
\gamma_2 &= \rho_h^{-1}\left\langle \rho D\right\rangle, \\
\gamma_3 &= \rho_m^{-1}\left\langle \rho T\right\rangle - \rho_m^{-2}\left\langle \rho E\right\rangle^2, \\
\gamma_4 &= \rho_h^{-1}\left\langle \rho Q\right\rangle + \left\langle \rho^{-1}F\right\rangle\left\langle \rho D\right\rangle + \rho_m^{-1}\left\langle \rho S\right\rangle - \rho_m^{-1}\rho_h^{-1}\left\langle \rho E\right\rangle\left\langle \rho D\right\rangle, \\
\gamma_5 &= \left\langle \rho D\right\rangle\left\langle \rho^{-1}H\right\rangle + \rho_h^{-1}\left\langle \rho R\right\rangle,
\end{aligned}$$

where the functions $A(\hat{y})$, $B(\hat{y})$, and $C(\hat{y})$ are defined in (18a); $D(\hat{y})$, $E(\hat{y})$, $F(\hat{y})$, and $H(\hat{y})$ are defined in (25); and $Q(\hat{y})$, $R(\hat{y})$, $S(\hat{y})$, $T(\hat{y})$, $U(\hat{y})$, $V(\hat{y})$, and $W(\hat{y})$ are given by

$$\begin{aligned}
Q(\hat{y}) &= [\![K^{-1}K_h\left(N - CK_h\left\langle K^{-1}F\right\rangle\right) - \rho^{-1}\rho_h\left(N - C\rho_h\left\langle \rho^{-1}F\right\rangle\right) - I]\!],\\
R(\hat{y}) &= [\![K^{-1}K_h\left(P - CK_h\left\langle K^{-1}H\right\rangle\right) - \rho^{-1}\rho_h\left(P - C\rho_h\left\langle \rho^{-1}H\right\rangle\right) - J]\!],\\
S(\hat{y}) &= [\![K^{-1}K_h\left(P - CK_h\left\langle K^{-1}H\right\rangle\right) - L]\!],\\
T(\hat{y}) &= [\![K^{-1}K_h\left(N - CK_h\left\langle K^{-1}F\right\rangle\right) - M]\!],\\
U(\hat{y}) &= [\![\rho\rho_m^{-1}\left(M - B\rho_m^{-1}\left\langle \rho E\right\rangle\right) - N]\!],\\
V(\hat{y}) &= [\![\rho A\left\langle \rho^{-1}F\right\rangle + \rho\rho_h^{-1}I + \rho\rho_m^{-1}\left(L - B\rho_h^{-1}\left\langle \rho D\right\rangle\right) - P]\!],\\
W(\hat{y}) &= [\![\rho A\left\langle \rho^{-1}H\right\rangle + \rho\rho_h^{-1}J]\!].
\end{aligned}$$

Finally,

$$\begin{aligned}
\tilde{A}(\hat{y}) = &\Big[\!\Big[K^{-1}K_h\Big(W - K_h\left\langle K^{-1}W\right\rangle - K_hH\left\langle K^{-1}H\right\rangle + K_h^2\left\langle K^{-1}H\right\rangle^2\Big)\\
&\quad - \rho^{-1}\rho_h\Big(W - \rho_h\left\langle \rho^{-1}W\right\rangle - \rho_hH\left\langle \rho^{-1}H\right\rangle + \rho_h^2\left\langle \rho^{-1}H\right\rangle^2\Big)\Big]\!\Big],\\
\tilde{B}(\hat{y}) = &[\![\rho A\left\langle \rho^{-1}W\right\rangle + \rho J\left\langle \rho^{-1}H\right\rangle + \rho\rho_h^{-1}\tilde{A}]\!].
\end{aligned}$$

In order to compute these functions, one must specify K and ρ. Below we give further details for the piecewise-constant medium (2) and the sinusoidal medium (41).

B.1. Piecewise-constant medium. For the piecewise-constant medium, it is easy to obtain the fast-variable functions and the coefficients in closed form; however, most of them are too cumbersome to present here. Therefore, we just show the coefficients of the first nonzero correction and refer to http://github.com/ketch/effective_dispersion_RR for Mathematica files where the rest of the coefficients can be found. The coefficients of the first nonzero correction for the piecewise medium are

$$\begin{aligned}
\alpha_1 &= \frac{-\left(K_A - K_B\right)}{192K_m^2}\cdot\frac{\left(Z_A^2 - Z_B^2\right)}{\rho_m}\lambda^2,\\
\alpha_2 &= \frac{-\left(K_A - K_B\right)}{192K_m^2}\cdot\frac{\left(c_A^2 - c_B^2\right)}{\rho_m^{-1}}\lambda^2,\\
\beta_1 &= \frac{\left(\rho_A - \rho_B\right)}{192K_m}\cdot\frac{\left(Z_A^2 - Z_B^2\right)}{\rho_m^2}\lambda^2,\\
\beta_2 &= \frac{\left(\rho_A - \rho_B\right)}{192K_m}\cdot\left(c_A^2 - c_B^2\right)\lambda^2,\\
\gamma_1 &= \frac{-\left(\rho_A - \rho_B\right)}{192K_m}\cdot\frac{\left(Z_A^2 - Z_B^2\right)}{\rho_m^2}\lambda^2,\\
\gamma_2 &= \frac{-\left(\rho_A - \rho_B\right)}{192K_m}\cdot\left(c_A^2 - c_B^2\right)\lambda^2.
\end{aligned}$$

B.2. Sinusoidal medium. For the sinusoidal medium and for more general y-periodic media, it is difficult to find closed expressions for the fast-variable functions and for the coefficients. Therefore, we solve the boundary value problems and compute the coefficients numerically. Details can be found at http://github.com/ketch/effective_dispersion_RR. The files available there can easily be modified to produce coefficients for other media.

The numerically computed coefficients for the sinusoidal medium are (taking $\lambda = 1$)

$$\begin{aligned}
\alpha_1 &= 2.2656 \times 10^{-10}, & \alpha_2 &= -1.3208 \times 10^{-2},\\
\alpha_3 &= -1.8927 \times 10^{-11}, & \alpha_4 &= -1.8172 \times 10^{-4},\\
\alpha_5 &= 1.3398 \times 10^{-3}, & \alpha_6 &= 6.0711 \times 10^{-6},\\
\beta_1 &= 2.9249 \times 10^{-4}, & \beta_2 &= -1.1033 \times 10^{-2},\\
\beta_3 &= -5.6345 \times 10^{-7}, & \beta_4 &= -2.3474 \times 10^{-5},\\
\beta_5 &= 1.1465 \times 10^{-3}, & \beta_6 &= 6.9060 \times 10^{-6},\\
\gamma_1 &= 2.2656 \times 10^{-10}, & \gamma_2 &= 1.2843 \times 10^{-2},\\
\gamma_3 &= -1.8927 \times 10^{-11}, & \gamma_4 &= -1.3391 \times 10^{-3},\\
\gamma_5 &= -1.6986 \times 10^{-4}.
\end{aligned}$$

Acknowledgments. The authors thank the referees for their comments that significantly improved this paper. Research reported in this publication was supported by the King Abdullah University of Science and Technology (KAUST).

REFERENCES

[1] W. Chen and J. Fish, *A dispersive model for wave propagation in periodic heterogeneous media based on homogenization with multiple spatial and temporal scales*, J. Appl. Mech., 68 (2001), pp. 153–161.

[2] C. Conca and M. Vanninathan, *Homogenization of periodic structures via bloch decomposition*, SIAM J. Appl. Math., 57 (1997), pp. 1639–1659.

[3] J. Fish and W. Chen, *Higher-order homogenization of initial/boundary-value problem*, J. Eng. Mech., 127 (2001), pp. 1223–1230.

[4] T. R. Fogarty and R. J. LeVeque, *High-resolution finite-volume methods for acoustic waves in periodic and random media*, J. Acoustical Soc. Amer., 106 (1999), pp. 17–28.

[5] J.-P. Fouque, J. Garnier, G. Papanicolau, and K. Solna, *Wave Propagation and Time Reversal in Randomly Layered Media*, Stoch. Model. Appl. Probab. 56, Springer, New York, 2007.

[6] D. I. Ketcheson, K. T. Mandli, A. J. Ahmadia, A. Alghamdi, M. Quezada de Luna, M. Parsani, M. G. Knepley, and M. Emmett, *PyClaw: Accessible, extensible, scalable tools for wave propagation problems*, SIAM J. Sci. Comput., 34 (2012), pp. C210–C231.

[7] D. I. Ketcheson, M. Parsani, and R. J. LeVeque, *High-order wave propagation algorithms for hyperbolic systems*, SIAM J. Sci. Comput., 35 (2013), pp. A351–A377.

[8] D. I. Ketcheson and M. Quezada de Luna, *Diffractons: 2D solitary waves in layered periodic media*, SIAM J. Multiscale Modeling Simulation, to appear; also available online from arXiv:1312.4122, 2013.

[9] R. J. LeVeque, *Wave propagation algorithms for multidimensional hyperbolic systems*, J. Comput. Phys., 131 (1997), pp. 327–353.

[10] R. J. LeVeque and D. H. Yong, *Solitary waves in layered nonlinear media*, SIAM J. Appl. Math., 63 (2003), pp. 1539–1560.

[11] M. Quezada de Luna and D. I. Ketcheson, *Numerical simulation of cylindrical solitary waves in periodic media*, J. Sci. Comput., 58 (2014), pp. 672–689.

[12] F. Santosa and W. Symes, *A dispersive effective medium for wave propagation in periodic composites*, SIAM J. Appl. Math., 51 (1991), pp. 984–1005.

[13] L. Trefethen, *Spectral Methods in MATLAB*, SIAM, Philadelphia, 2000.

[14] D. H. Yong and J. Kevorkian, *Solving Boundary-Value Problems for Systems of Hyperbolic Conservation Laws with Rapidly Varying Coefficients*, Stud. Appl. Math. 108, 2002, pp. 259–303.